J. Am. Soc. Mass Spectrom. (2017) 28:182–189
DOI: 10.1007/s13361-016-1510-1

RESEARCH ARTICLE

Stereochemical Sequence Ion Selectivity: Proline versus Pipecolic-acid-containing Protonated Peptides

Maha T. Abutokaikah, Shanshan Guan, Benjamin J. Bythell

Department of Chemistry and Biochemistry, University of Missouri, St. Louis, MO 63121, USA

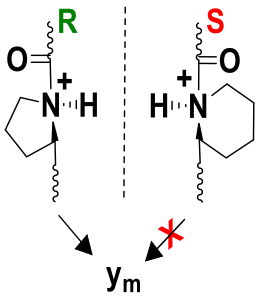

Abstract. Substitution of proline by pipecolic acid, the six-membered ring congener of proline, results in vastly different tandem mass spectra. The well-known proline effect is eliminated and amide bond cleavage C-terminal to pipecolic acid dominates instead. Why do these two ostensibly similar residues produce dramatically differing spectra? Recent evidence indicates that the proton affinities of these residues are similar, so are unlikely to explain the result [Raulfs et al., J. Am. Soc. Mass Spectrom. **25**, 1705–1715 (2014)]. An additional hypothesis based on increased flexibility was also advocated. Here, we provide a computational investigation of the "pipecolic acid effect," to test this and other hypotheses to determine if theory can shed additional light on this fascinating result. Our calculations provide evidence for both the increased flexibility of pipecolic-acid-containing peptides, and structural changes in the transition structures necessary to produce the sequence ions. The most striking computational finding is inversion of the stereochemistry of the transition structures leading to "proline effect"-type amide bond fragmentation between the proline/pipecolic acid-congeners: R (proline) to S (pipecolic acid). Additionally, our calculations predict substantial stabilization of the amide bond cleavage barriers for the pipecolic acid congeners by reduction in deleterious steric interactions and provide evidence for the importance of experimental energy regime in rationalizing the spectra.

Keywords: Mass spectrometry, Collision-induced dissociation, Proteomics, Density functional theory

Received: 25 May 2016/Revised: 12 September 2016/Accepted: 15 September 2016/Published Online: 11 October 2016

Introduction

Tandem mass spectrometry is the key technology utilized in peptide sequencing and proteomics [1–3]. Typically, individual peptides are isolated prior to collisional activation and identification of sequence is subsequently achieved based on the detected mass-to-charge (m/z) ratios corresponding to the charged fragments and the precursor protonated peptide. Ideally, collision-induced dissociation (CID) initiates cleavage of the amide bonds to produce series of b_n ions if the N-terminal fragment keeps the charge, y_m ions if the C-terminal fragment keeps the charge, or a mixture of the two (for a peptide of length N = n + m) [4–6]. The relative abundance of the product ions depends on the peptide sequence, charge state, instrument type, and the specific conditions under which the experiments were performed [3, 5, 7–13]. Certain amino acid residues strongly enhance specific types of bond cleavage [10–12, 14–16]. Among this suite of residue-specific chemistries is that associated with proline, P (Scheme 1a). In the well-documented "proline effect" [17–24], a strong preference for amide bond cleavage N-terminal to proline residues is observed. This chemistry results in enhanced prevalence of the y_m ion peak with the proline residue situated at its N-terminus with concomitant suppression of the complementary b_n ion (Scheme 2). Proline is unique among the 20 commonly occurring amino acids in that it contains a secondary amine, in a 5-membered ring at its N-terminus (Scheme 1a). Consequently, once involved in an amide bond, it becomes a tertiary amine. Pipecolic acid, Pip, is the 6-membered ring congener of proline (Scheme 1b) and has its own residue-specific chemistry, the "pipecolic acid effect" [20]. Despite obvious structural similarity between proline and pipecolic acid, the two effects (residues) result in vastly different mass spectra of otherwise identical protonated peptide sequences [18, 20].

Pipecolic acid has been shown to promote the dominant formation [18, 20] of specific b_n peaks rather than y_m peaks (Scheme 3). Furthermore, the amide bond that is cleaved differs in the pipecolic acid effect; the amide bond C-terminal to the

Electronic supplementary material The online version of this article (doi:10.1007/s13361-016-1510-1) contains supplementary material, which is available to authorized users.

Correspondence to: Benjamin J. Bythell; *e-mail:* bythellb@umsl.edu

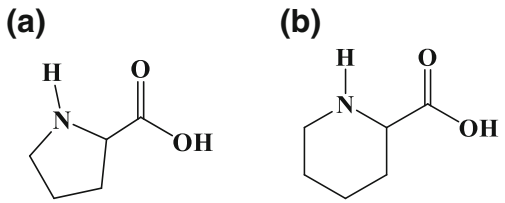

Scheme 1. Schematic of (**a**) proline, (**b**) pipecolic acid

pipecolic acid residue is broken. Raulfs et al. [20] demonstrated this phenomenon in their recent paper by utilizing combined experimental and theoretical comparisons of singly protonated pentapeptides, $[AAXAA + H]^+$, where the identity of X was systematically varied [X = P, Pip, *N*-methylalanine, azetidine-2-carboxylic acid (the 4-membered ring analogue); A = alanine]. Parallel to earlier work [18], they showed that proline and azetidine-2-carboxylic acid behave similarly and give rise to dominant y_3 peaks [20], whereas pipecolic acid and *N*-methylalanine promote the dominant formation of b_3 peaks. Swapping the alanine residues for other aliphatic residues had minimal effect on this result [18, 20]. Furthermore, when peptides containing *both* the Pip and P residues were analyzed, the dominant products observed were always the b_n peaks corresponding to the position of the Pip residue (i.e., for $[APipAPA + H]^+$, the b_2 peak, for $[AAPipPA + H]^+$ the b_3 peak, and for $[APAPipA + H]^+$ the b_4 peak).

Additionally, Raulfs et al. [20] provided computational estimates of the proton affinities of the residues, which showed that Pip had a very similar proton affinity to P. Previously, the same corresponding author had analogous experimental findings [25]. Extrapolating on this basis [17, 20], the results could not be rationalized based solely on the basicity of the prolyl nitrogen as had previously been argued [18]. Consequently, Raulfs et al. [20] attributed the result to greater flexibility of the Pip 6-membered ring "which allows for peptides conformations that promote favorable transfer of the mobile proton to the amide C-terminal to the Pip/*N*-methylalanine residue." This flexibility-based explanation essentially argues for a proton-transfer-limited reactivity, whereby the ability to protonate each specific amide nitrogen can be used as a surrogate for the barrier to the subsequent sequence ion formation. This is broadly consistent with the mobile proton model [15, 26, 27], and has been specifically argued for by Haeffner et al. [28]. Consequently, the specific question of what the transition structures look like and the product ion energies were not addressed explicitly.

These interesting findings [20] motivated the present computational investigation into the mechanisms of fragmentation of these related systems. Here, we provide a systematic computational study of the fragmentation chemistry of $[AAXA_o + H]^+$ peptides; where X = P/Pip and o = 0, 1, 2, 3 to test the flexibility hypothesis. We examine the relative energies of the critical transition structures, product ions, and neutrals as a function of peptide length to help explain the chemistry in play. Predictions based on the progression in leaving group size, composition, and proton affinities are also provided [24, 29–31].

Theoretical Methods

Density functional calculations of minima, and product ions and neutrals were performed with the Gaussian 09 suite of programs [32] at the M06-2X/6-31+G(d,p) level of theory [33, 34]. Multiple conformers of each protonation site were examined for each system. Our typical protonation site labeling convention is illustrated in Supplementary Scheme S1. Multiple transition structures (TSs) were calculated. Minima were confirmed by vibrational analysis (all real frequencies) and TSs were also examined in this manner (one imaginary frequency). The reaction pathway through the TSs was determined by intrinsic reaction coordinate (IRC) calculations with up to 18 steps in each direction. The terminating points of these calculations (one on product side, one on reactant side) were then optimized further to determine the exact minima connected by each specific reaction path. Estimates of the proton affinities of the leaving groups were determined as the difference between the zero-point energy-corrected M06-2X/6-31+G(d,p) total electronic energies (0 K) of the protonated and neutral forms of the potential b_n and y_m ions, respectively.

In response to a reviewer's request, we added calculations on the $[AA(D\text{-}Proline)AA + H]^+$ system to the analysis. In response to a second reviewer's request, we provided

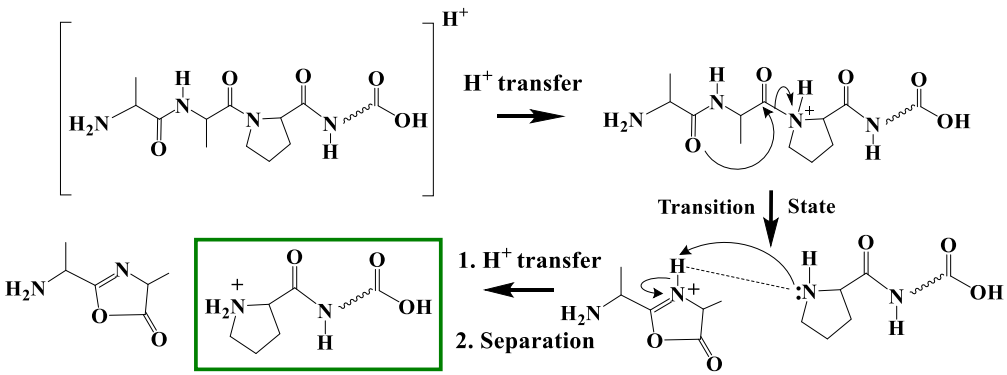

Scheme 2. Generic b_2-$y_{(N-2)}$ mechanism of proline-containing peptides to form $y_{(N-2)}$ product ions

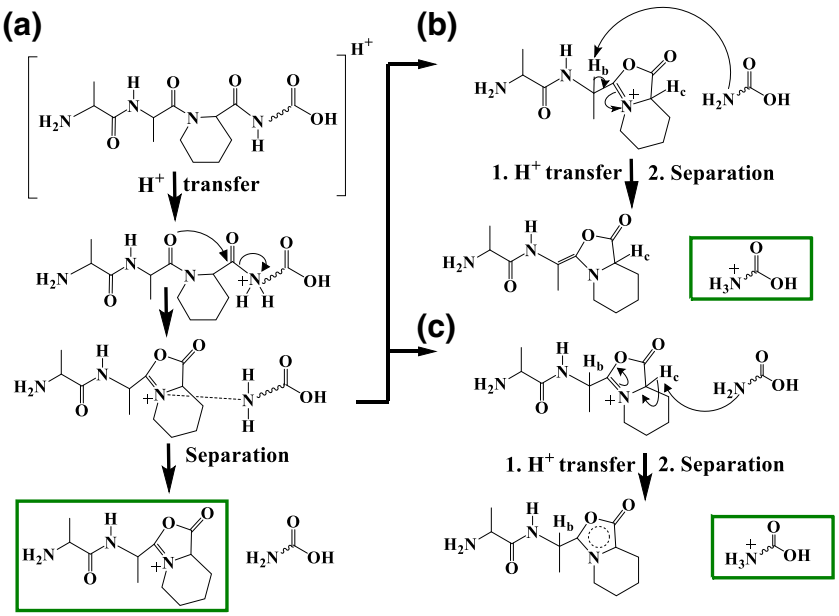

Scheme 3. Generic fragmentation mechanism of pipecolic-acid-containing protonated peptides: (**a**) formation of b_3 product ions, (**b**) proton transfer of the alanyl C_α H^+ to form $y_{(N-3)}$ product ions (within the proton-bound dimer), (**c**) alternate proton transfer reaction from the oxazolone ring pipecolic acid C_α H^+ to form $y_{(N-3)}$ product ions

additional calculations at the M06-2X/6-311++G(2d,p), B3LYP/6-31+G(d,p), and B3LYP/6-311++G(2d,p) levels of theory for the $[AAXAA+H]^+$ systems.

Results and Discussion

Protonation Energetics

We calculated the potential energy surface of $[AAXA_o + H]^+$ peptides, where X = P/Pip and o = 0, 1, 2, 3. Our data are normalized to the lowest energy, all *trans* amide bond structure, labeled as the global minimum, GM, in each case. We note that in analogy with recent work from the Clemmer [35–37] and Paizs groups [24] that *cis* conformations are also potentially competitive (Supplementary Tables S1–S8). Our calculations predict the protonation site of the global minimum will vary as a function of peptide length, but that this is consistent between the P/Pip forms (Supplementary Tables S1–S14). For example, based on the M06-2X calculations, the global minimum for both $[AAXAA + H]^+$ ions is protonated on the third oxygen, O3 (Supplementary Tables S1 and S2, Supplementary Figure S1). In some cases, a *cis* conformer is more energetically favorable than the corresponding *trans* global minimum. Again, this is consistent, irrespective of whether P/Pip is present. In agreement with the literature, protonation of an amide nitrogen requires additional energy [5, 8, 13, 21, 24, 28, 38–45]. A typical prerequisite to amide bond cleavage is protonation of the specific amide nitrogen that is to be cleaved, as this removes conjugation from the bond, reducing the bond order, and makes it easier to break [39, 41]. Our data do show that population of the third amide nitrogen site (N3, which is C-terminal to Pip/P) requires less energy (by >11 kJ mol^{-1}) for pipecolic-acid-containing peptides than it does for the analogous proline forms. This supports the hypothesis of increased flexibility of pipecolic acid enabling population of these sites [20]. For example, for $[AAPipAA + H]^+$ the reactive precursor structure protonated at N3 (71.9 kJ mol^{-1}, Supplementary Table S2) can be readily populated via proton transfer from a proximal O3 protonated structure through a TS requiring only 89 kJ mol^{-1}. Prior theory [45] and experiment [46] indicate that population of these sites will have substantially greater rate constants than those of subsequent higher energy amide bond cleavage barriers.

The evidence for the flexibility-based explanation being the *sole* cause of the difference in chemistry is contradicted by the additional finding that population of the second amide nitrogen site, N2, at P/Pip, is predicted to require *much less energy* than N3. If the amide bond cleavage TSs are rate-limiting, and follow directly from the amide nitrogen protonation energetics [28], then the b_2-y_{N-2} pathway should be universally favored over the b_3-y_{N-3} reaction. Consequently, there would be little difference in the spectra of protonated peptides containing P/Pip. The preponderance of experimental data [17, 20] and our calculations indicate this is not the case. Consequently, we need additional information on the relative energies of the competing TSs to determine if they are the cause of the differing reactivities.

Amide Bond Cleavage TSs

The mechanism of enhanced y_m ion formation via the proline effect is illustrated in Scheme 2 [24]. The prevailing mechanism of fragmentation of pipecolic-acid-containing protonated peptides differs (Scheme 3a). While pipecolic-acid-containing

protonated peptides typically generate b_n ions, formation of the complementary y_m ions is, in principle, also possible. This reaction requires abstraction of a non-mobile proton from the fixed charge N-terminal fragment. There are two likely candidate sites for this abstraction to occur from (Scheme 3b and c): the C_α proton of the preceding alanine residue or the fixed-charge oxazolone ring [47]. As neither proton is mobile, these are also potentially rate-limiting transition structures that might explain the lack of an y_{N-3} ion peak (Scheme 3b). First, however, we need to discuss the relative energetics of the amide bond cleavage reactions of $[AAXA_o + H]^+$ peptides as without this step occurring, discussion of proton-bound dimer chemistry is moot.

In agreement with the prior experimental [18, 20, 21, 24] and theoretical [20, 21, 24] findings, and the proline effect in general, our calculations predict the b_2-y_m amide bond cleavage TS to be consistently less energetically demanding for $[AAPA_o + H]^+$ peptides than the b_3-y_{N-3} amide bond cleavage (Table 1, Supplementary Table S1). The degree to which this is the case varies, but is consistently >20 kJ mol^{-1}. The general mechanism is described in Scheme 2 and an example TS is shown in Figure 1 for $[AAPAA + H]^+$. Following this relatively facile amide bond cleavage, we would expect the high proton affinity [25] of the proline-terminated fragment (932, 957, 977, 989 kJ mol^{-1} for P, PA, PAA, PAAA, respectively, Table 2) relative to the neutral alanylalanine-oxazolone structure (912 kJ mol^{-1}, see also [48]) to result in proton transfer from the oxazolone ring nitrogen to form the y_m ion prior to complex separation. This process becomes increasingly likely as the size and, thus, proton affinity of the PA_o fragment formed increases. If the b_3-y_{N-3} amide bond cleavage reaction occurs at all (Supplementary Scheme S2, Figure 2a), the product distribution will again be affected by the proton affinities of the neutral forms of the fragments. However, for this to be relevant, an energetically feasible means of proton abstraction must be available to the C-terminal fragment (Supplementary Scheme S2, Supplementary Table S1, and Supplementary Figure S3) [47]. Our calculations indicate that the two potential proton abstraction reactions are equi-energetic with the amide bond cleavage barrier so they should not limit the reaction significantly. Poutsma and coworkers' experiments on $[AAPAA + H]^+$ show [20] a tiny b_3 peak (~1% relative abundance) consistent with the proton affinity of the b_3 neutral (≥966 kJ mol^{-1} Table 2) being substantially greater than AA. The product distribution should be much more even for the b_3-y_{N-3} reaction of $[AAPAAA + H]^+$ as AAA has a much more similar proton affinity (962 kJ mol^{-1}, Table 2).

Table 1. Transition Structure Relative Energies ($\Delta E_{el+ZPE,0K}$ (ΔG_{298K})/kJ mol^{-1}) of $[AAXA_o + H]^+$, where X = P/Pip and o = number of alanine residues for the b_2 $-y_{(N-2)}$ and b_3 $-y_{(N-3)}$ pathways

X	o	b_2 $-y_{N-2}$	b_3 $-y_{N-3}$
P	0	*122.0 (126.4)*	*143.3 (148.4)*
Pip	0	*110.7 (113.6)*	*137.3 (141.3)*
P	1	*113.2 (111.4)*	*145.6 (149.2)*
Pip	1	*100.1 (103.1)*	*91.8 (97.8)*
P	2	*120.9 (117.0)*	*149.0 (144.5)*
Pip	2	*107.8 (109.1)*	*101.9 (104.8)*
P	3	*119.3 (122.0)*	*143.4 (148.3)*
Pip	3	*112.5 (109.9)*	*102.1(98.9)*

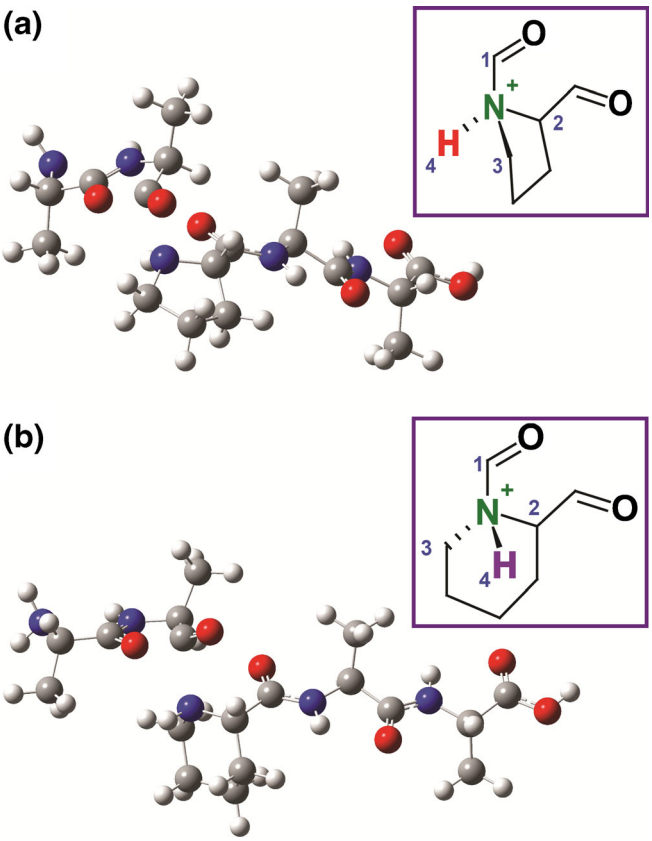

Figure 1. The b_2-y_3 transition structures at the M06-2X/6-31+G(d,p) level of theory; (**a**) $[AAPAA+H]^+$, (**b**) $[AAPipAA + H]^+$. **Inset**: standard projections illustrating the stereochemical consequences of protonation either below the ring as is favored in the P-containing analyte b_2-y_3 TSs: (**a**) R stereochemistry at the prolyl amide nitrogen, or above the ring as is favored in the Pip-containing analyte b_2-y_3 TSs: (**b**) S stereochemistry at the pipecolic acidyl amide nitrogen. Numbers indicate the priority of substituents in assigning configuration

Our calculations are also in general agreement with the experimental data underlying the pipecolic acid effect. The M06-2X/6-31+G(d,p) transition structure calculations predict that the $[AAPipA_o + H]^+$ (o = 1–3) peptides should generally favor the b_3-y_{N-3} amide bond cleavage over the b_2-y_m amide bond cleavage reaction (Table 1, Supplementary Table S2). For example, the $[AAPipAA + H]^+$ system investigated by Poutsma and coworkers experimentally [20] produced b_3 and y_3 peaks in an approximately 4:1 ratio. The energy of the b_3-y_2 amide bond cleavage TS [$\Delta E_{el+ZPE,0K}$ (ΔG_{298K}) = 101.9 (104.8) kJ mol^{-1}, Figure 2b) is lower than, but similar to, the b_2-y_3 TS energy (107.8 (109.1) kJ mol^{-1}, Figure 1b). The most facile subsequent proton abstraction reaction from the oxazolone ring (Scheme 3c, Table 2) is less energetically demanding (96 kJ mol^{-1}) than the amide bond cleavage. However, the neutral b_3 oxazolone generated from this TS has substantially greater proton affinity (1052 kJ mol^{-1}) than AA (923 kJ mol^{-1}) which, consistent with the lack of any y_2 peak,

Table 2. Calculated Gas-Phase Proton Affinities of the Various Neutrals Present in Post Amide Bond Cleavage Proton-Bound Dimer

Pathway	Neutral	MS/MS ion	Proton Affinity/ kJ mol^{-1}
$b_2 - y_{(N-2)}$	AA oxazolone	b_2	911.6
$b_2 - y_{(N-2)}$	P	y_1	931.6
$b_2 - y_{(N-2)}$	PA	y_2	957.4
$b_2 - y_{(N-2)}$	PAA	y_3	976.8
$b_2 - y_{(N-2)}$	PAAA	y_4	989.0
$b_2 - y_{(N-2)}$	Pip	y_1	931.7
$b_2 - y_{(N-2)}$	PipA	y_2	962.4
$b_2 - y_{(N-2)}$	PipAA	y_3	975.2
$b_2 - y_{(N-2)}$	PipAAA	y_4	982.7
$b_3 - y_{(N-3)}$	Alanyl C_α H^+ deprotonated neutral AAP oxazolone	b_3	966.3
$b_3 - y_{(N-3)}$	Proline C_α H^+ deprotonated neutral AAP oxazolone	b_3	998.2
$b_3 - y_{(N-3)}$	Alanyl C_α H^+ deprotonated neutral AAPip oxazolone	b_3	1008.1
$b_3 - y_{(N-3)}$	Proline C_α H^+ deprotonated neutral AAPip oxazolone	b_3	1051.9
$b_3 - y_{(N-3)}$	H_2O	H_3O^+	689.0
$b_3 - y_{(N-3)}$	A	y_1	889.8
$b_3 - y_{(N-3)}$	AA	y_2	922.6
$b_3 - y_{(N-3)}$	AAA	y_3	961.6

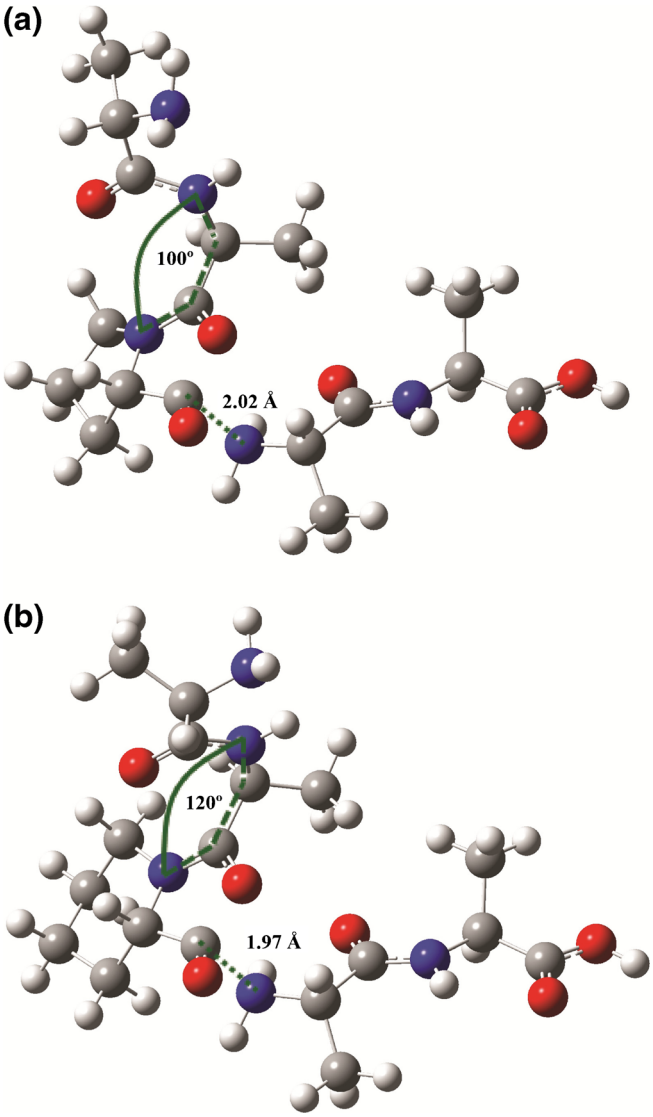

Figure 2. (**a**) b_3-y_2 TS of $[AAPAA + H]^+$ and (**b**) b_3-y_2 TS of $[AAPipAA + H]^+$ at M06-2X/6-31+G (d,p) level of theory. Critical bond lengths and dihedral angles are provided for contrast

makes this transformation very unlikely. The $[AAPip + H]^+$ analyte is an exception in that it is predicted to yield a y_1 peak rather than a b_3. Here, the b_2-y_1 TS is > 25 kJ mol^{-1} *lower* than the b_3-H_2O TS. This is due to water being a comparatively poor leaving group [49], with limited hydrogen-bonding capability to stabilize the TS relative to alanine or polyalanine. Consequently, a y_1 ion, $[Pip + H]^+$, is predicted to be formed and subsequently detected, consistent with pipecolic acid having greater proton affinity than neutral AA oxazolone (Table 2).

Proline versus Pipecolic Acid-Transition Structure Stereochemistry Differences

The lowest energy amide bond cleavage barriers for the pipecolic-acid-containing protonated peptides are consistently lower than their proline-containing congeners. This broadly agrees with Poutsma and co-workers' [20] data on direct competition between P/Pip enhanced fragmentations in a single protonated peptide. These authors found that the b_n peak with C-terminal Pip was always the base peak (i.e., the "pipecolic acid effect" appeared to be stronger than the "proline effect" under their experimental conditions). Broadly, the Pip residue's increased size and flexibility enables superior stabilization of the key transition structures and intermediates necessary to form the requisite products. How does this happen?

Although the lowest energy b_3-y_{N-3} TSs are quite similar, differences do exist. We utilize the $[AAXAA + H]^+$ systems to illustrate this. Our density functional calculations predict two major areas of difference: (1) a longer critical amide bond length for the prolyl form (2.02 Å) versus the pipecolic acid form (1.97 Å), and (2) a rotation of the N-terminus of the oxazolone-ring, which is being formed (dihedral angle N_P-$C(O)_{A2}$-C_{A2}-N_{A2} = 100°: N_{Pip}-$C(O)_{A2}$-C_{A2}-N_{A2} = 120°) resulting in a decreased degree of unfavorable steric interactions for $[AAPipAA + H]^+$ (interaction distances increase 0.1–0.25 Å, Figure 2). Although these changes are relatively subtle, the differences in the corresponding b_2-y_{N-2} TSs are much greater.

Table 3. Summary Table of Separated Product Energies of $[AAPAA + H]^+$ calculated at the M06-2X/6-31+G (d,p) Level of Theory

Products	E_{el}/H	E_{el+ZPE}/H	$\Delta E_{el+ZPE,0K}$ /kJ mol^{-1}	ΔH_{298}/ kJ mol^{-1}	ΔG_{298}/ kJ mol^{-1}	ΔS_{298}/ J mol^{-1}
$b_2^+ + PAA$	–1390.293488	–1389.798506	225.7	226.7	162.5	215.6
Neutral AA oxazolone + y_3^+	–1390.320506	–1389.823335	160.5	160.4	102.2	195.2
$b_3^+ + AA$	–1390.303757	–1389.808777	198.7	200.0	140.8	198.4
Alanyl C_α H^+ deprotonated *AAP* oxazolone + y_2^+	–1390.287038	–1389.792131	242.4	242.9	184.8	195.0
Proline C_α H^+ deprotonated *AAP* oxazolone + y_2^+	–1390.275114	–1389.779980	274.3	274.8	217.5	191.9

The switch from proline to pipecolic acid results in inversion of the stereochemistry of the critical b_2-y_{N-2} TSs (Figure 1, Supplementary Figure S4). The necessity of considering stereochemistry arises from protonation of the ring nitrogen (N2) resulting in R or S stereochemistry depending on whether the added proton is "above or below" the ring (Supplementary Figure S4). This was recognized previously by Bleiholder et al. [24], who found the lowest energy critical amide bond cleavage b_3-y_2 TS of the $[AAAPA + H]^+$ peptide to be ~25 kJ mol^{-1} lower for the R stereo configuration. Consistent with this finding, our $[AAPA_o + H]^+$ systems also preferentially favor the R stereo configuration for the analogous b_2-y_{N-2} TSs (Figure 1a, Supplementary Figure S4). In marked contrast, however, the $[AAPipA_o + H]^+$ congeners lowest energy TSs all have S stereochemistry (Figure 1b, Supplementary Figure S4). Why the difference? The bulkier, 6-membered ring of Pip is far less sterically hindered by interactions with the methyl group of the N-terminal alanine in the S configuration. Essentially, the ring is placed perpendicular to the planar C-terminal end of the protonated peptide and thus limits deleterious interactions with the alanine methyl group. The combination of the relative destabilization of the most competitive b_2-y_{N-2} TSs coupled to the structural adjustments that stabilize the b_3-y_{N-3} TSs provides the explanation for the change in major product from y_{N-2} peaks for the proline-containing systems to b_3 peaks for those containing a pipecolic acid residue (i.e., the pipecolic acid effect). As these structural effects are not independent and occur simultaneously, it's not possible to single out one as the sole cause.

Product Energies and Fragmentation Regime: Why Do We Detect the Peaks We Detect?

It should be explicitly noted that the experimental data to which we are comparing our calculations was collected at energies *substantially above* the threshold for fragmentation. Consequently, the best measure of the reaction propensities we provide is the Gibbs free energy, ΔG_{298K}, as this incorporates both enthalpic and entropic contributions, which are important in this energy regime. If, instead, we were predicting the behavior at threshold ($\Delta E_{el+ZPE,0K}$), the enthalpic barrier (TS or products, whichever is higher) would be most relevant. This is particularly pertinent for the present systems, as at threshold, all of these reactions are product-limited. Consequently, at energies barely above threshold, we would expect a different experimental result: $[AAPAA + H]^+$ and $[AAPipAA + H]^+$ should both lead to predominant y_3 peaks, as the lowest energy thresholds ($\Delta E_{el+ZPE,0K}$) are 160.5 and 136.8 kJ mol^{-1}, respectively, for neutral AA-oxazolone and y_3^+ (Tables 3 and 4). As the degree of activation increased further above the threshold energy, the Gibbs free energy, ΔG, (TS or products, whichever is higher) becomes the most important quantity. It is important to recognize that the ΔG of the TS and products *vary at different rates* with temperature. This is because the combined entropy of two separated gas-phase species (one ion, one neutral here) adds up to a substantially larger entropy than that of a single gas-phase ion (like the pertinent TS), i.e., the ΔS term is large and positive for the products (~190 J mol^{-1}, Tables 3 and 4), in comparison to the TS. So at very high temperature, very few dissociation reactions will be product-limited. Practically, this means that if the ΔG of the products is greater than that of the TS at threshold, as in the b_3-y_2 pathway of $[AAPipAA + H]^+$, this situation will invert at higher effective temperature, enabling b_3 ion production to become increasingly more competitive. The experiments analyzed here [17, 20] were performed under such conditions, thereby enabling the resulting spectra to favor the b_3-y_2 pathway products for pipecolic-acid-containing systems (producing b_3 ions here).

Exploring Additional Stereochemical Differences with [AA(D-Proline)AA + H]$^+$

Raulfs et al. [20] also examined the effect of substitution of a D-proline residue in place of the L-proline or L-pipecolic acid

Table 4. Summary Table of Separated Product Energies of $[AAPipAA + H]^+$ Calculated at the M06-2X/6-31+G (d,p) Level of Theory

Products	E_{el}/H	E_{el+ZPE}/H	$\Delta E_{el+ZPE,0K}$ /kJ mol^{-1}	ΔH_{298}/ kJ mol^{-1}	ΔG_{298}/ kJ mol^{-1}	ΔS_{298}/ J mol^{-1}
$b_2^+ + PipAA$	–1429.596581	–1429.071768	200.4	200.5	143.7	190.6
Neutral AA oxazolone + y_3^+	–1429.622845	–1429.095995	136.8	136.4	81.8	183.1
$b_3^+ + AA$	–1429.609360	–1429.084486	167.1	168.0	112.7	185.6
Alanyl C_α H^+ deprotonated *AAPip* oxazolone + y_2^+	–1429.576868	–1429.051920	252.6	253.1	196.8	188.8
Pipecolic acid C_α H^+ deprotonated *AAPip* oxazolone + y_2^+	–1429.577787	–1429.053231	249.4	277.7	232.3	151.1

residues, $[AA(D\text{-}Proline)AA + H]^+$. This system provided yet another type of dominant fragmentation chemistry, producing the b_4 peak as the base peak. At approximately a quarter of this abundance is the y_3 peak, followed by a barely discernible b_3 peak. So the typical "proline-effect" fragmentation chemistry (b_2-y_3 pathway) is only the second most prevalent chemistry here. Consistent with this experimental finding, the lowest energy TS located was the b_4-y_1 at 94.9 (101.4) kJ mol^{-1} at the M06-2X/6-31+G(d,p) level of theory. The b_2-y_3 barrier was 122.5 (120.4) kJ mol^{-1} and finally the b_3-y_2 at 137.9 (138.3) kJ mol^{-1}. This is summarized in Supplementary Table S15 and the transition structures can be seen in Supplementary Figures S5 and S6. The b_4 ion product is also the most energetically favorable product based on our calculations (Supplementary Table S19), followed by the y_3 then the b_3, which again is consistent with the experimental data.

Larger Basis Sets and Alternate Model Chemistries

In response to a reviewer request, we also performed additional calculations at the M06-2X/6-311++G(2d,p), B3LYP/6-31+G(d,p), and B3LYP/6-311++G(2d,p) levels of theory for the $[AAXAA + H]^+$ systems. The findings of these calculations are generally consistent with the preceding explanation, so we have limited the discussion of these results to the present section and the Supporting Information. Increasing the M06-2X basis set size resulted in slightly lower TS barriers for both types of amide bond cleavage barrier (by ~10 and ~3.6 kJ mol^{-1} for the P and Pip congeners, respectively, Supplementary Tables S1, S2, S9, S12). Additionally, the larger basis set indicates that the b_2-y_{N-2} TS for the $[AAPipAA + H]^+$ system is much less entropically favorable than the b_3-y_{N-3} TS. Although this finding is entirely consistent with the experimental result (supports b_3 ion formation over y_3), the magnitude of change is a little surprising, particularly as the M06-2X structures are essentially identical at the two levels of theory. So we have a difference in the description of the frequencies provided between the two levels of theory. In comparison, both sets of B3LYP values are similar to each other. Both B3LYP basis sets lead to the b_2-y_{N-2} TS being more energetically and entropically demanding than the b_3-y_{N-3} TS, consistent with the experiment. The magnitude of the entropic difference is smaller than for the M06-2X/6-311++G(2d,p) data though. The other difference observed with the B3LYP functional is switching of relative energies of the lowest energy protonation sites from O3 to O2. Although notable, this has minimal impact on the general description of the dissociation chemistry.

Conclusions

Our calculations indicate that proline and pipecolic-acid-containing protonated peptides should have differing product ion distributions under low-energy CID conditions. The reasons for this are: (1) the previously hypothesized increased flexibility of pipecolic acid [20] enabling increased stabilization of the b_3-y_{N-3} amide bond cleavage transition structures relative to their proline-containing congeners; (2) a relative destabilization of the b_2-y_{N-2} transition structures, which manifests as a required inversion in the stereochemistry of the b_2-y_{N-2} transition structure from R (proline) to S (pipecolic acid). This is essentially due to the bulkier Pip side-chain imposing significant steric constraints. Additionally, we provide evidence for the further relevance of experimental energy regime when attempting to rationalize mass spectra and make predictions based on our calculations for related P/Pip systems' likely product distributions.

Acknowledgments

The authors acknowledge support for this work from start-up funds from the University of Missouri-St. Louis and a University of Missouri Research Board Grant. Calculations were performed at the University of Missouri Science and Technology Rolla, Missouri. M.T.A. thanks the Saudi Arabia Culture Mission for funding her graduate work. B.J.B. thanks Peter Armentrout for useful discussions.

References

1. Larsen, M.R., Roepstorff, P.: Mass spectrometric identification of proteins and characterization of their post-translational modifications in proteome analysis. Fresenius J. Anal. Chem. **366**, 677–690 (2000)
2. Aebersold, R., Goodlett, D.R.: Mass spectrometry in proteomics. Chem. Rev. **101**, 269–295 (2001)
3. Medzihradszky, K.F.: Peptide sequence analysis. Methods Enzymol. **402**, 209–244 (2005)
4. Biemann, K.: Contributions of mass spectrometry to peptide and protein structure. Biomed. Environ. Mass Spectrom. **16**, 99–111 (1988)
5. Paizs, B., Suhai, S.: Fragmentation pathways of protonated peptides. Mass Spectrom. Rev. **24**, 508–548 (2005)
6. Roepstorff, P., Fohlman, J.: Proposal for a common nomenclature for sequence ions in mass spectra of peptides. Biomed. Mass Spectrom. **11**, 601 (1984)
7. Papayannopoulos, I.A.: The interpretation of collision-induced dissociation tandem mass spectra of peptides. Mass Spectrom. Rev. **14**, 49–73 (1995)
8. Bythell, B.J., Csonka, I.P., Suhai, S., Barofsky, D.F., Paizs, B.: Gas-phase structure and fragmentation pathways of singly protonated peptides with N-terminal Arginine. J. Phys. Chem. B **114**, 15092–15105 (2010)
9. Kapp, E.A., Schuetz, F., Reid, G.E., Eddes, J.S., Moritz, R.L., O'Hair, R.A.J., Speed, T.P., Simpson, R.J.: Mining a tandem mass spectrometry database to determine the trends and global factors influencing peptide fragmentation. Anal. Chem. **75**, 6251–6264 (2003)
10. Huang, Y., Triscari, J.M., Tseng, G.C., Pasa-Tolic, L., Lipton, M.S., Smith, R.D., Wysocki, V.H.: Statistical characterization of the charge state and residue dependence of low-energy CID peptide dissociation patterns. Anal. Chem. **77**, 5800–5813 (2005)
11. Tabb, D.L., Huang, Y., Wysocki, V.H., Yates, J.R.: Influence of basic residue content on fragment ion peak intensities in low-energy collision-induced dissociation spectra of peptides. Anal. Chem. **76**, 1243–1248 (2004)
12. Tabb, D.L., Smith, L.L., Breci, L.A., Wysocki, V.H., Lin, D., Yates, J.R.: Statistical characterization of ion trap tandem mass spectra from doubly charged tryptic peptides. Anal. Chem. **75**, 1155–1163 (2003)
13. Armentrout, P.B., Heaton, A.L.: Thermodynamics and mechanisms of protonated diglycine decomposition: a computational study. J. Am. Soc. Mass Spectrom. **23**, 621–631 (2012)
14. Yu, W., Vath, J.E., Huberty, M.C., Martin, S.A.: Identification of the facile gas-phase cleavage of the Asp-Pro and Asp-Xxx peptide bonds in matrix-assisted laser desorption time-of-flight mass spectrometry. Anal. Chem. **65**, 3015–3023 (1993)

15. Wysocki, V.H., Tsaprailis, G., Smith, L.L., Breci, L.A.: Mobile and localized protons: a framework for understanding peptide dissociation. J. Mass Spectrom. **35**, 1399–1406 (2000)
16. Farrugia, J.M., Taverner, T., O'Hair, R.A.J.: Side-chain involvement in the fragmentation reactions of the protonated methyl esters of histidine and its peptides. Int. J. Mass Spectrom. **209**, 99–112 (2001)
17. Schwartz, B.L., Bursey, M.M.: Some proline substituent effects in the tandem mass spectrum of protonated pentaalanine. Biol. Mass Spectrom. **21**, 92–96 (1992)
18. Vaisar, T., Urban, J.: Probing the proline effects in CID of protonated peptides. J. Mass Spectrom. **31**, 1185–1187 (1996)
19. Breci, L.A., Tabb, D.L., Yates, J.R., Wysocki, V.H.: Cleavage N-terminal to proline: analysis of a database of peptide tandem mass spectra. Anal. Chem. **75**, 1963–1971 (2003)
20. Raulfs, M.D.M., Breci, L., Bernier, M., Hamdy, O.M., Janiga, A., Wysocki, V., Poutsma, J.C.: Investigations of the mechanism of the "proline effect" in tandem mass spectrometry experiments: the "pipecolic acid effect". J. Am. Soc. Mass Spectrom. **25**, 1705–1715 (2014)
21. Grewal, R.N., El Aribi, H., Harrison, A.G., Siu, K.W.M., Hopkinson, A.C.: Fragmentation of protonated tripeptides: the proline effect revisited. J. Phys. Chem. B **108**, 4899–4908 (2004)
22. Bernier, M.C., Chamot-Rooke, J., Wysocki, V.H.: R versus S fluoroproline ring substitution: trans/cis effects on the formation of b2 ions in gas-phase peptide fragmentation. Phys. Chem. Chem. Phys. **18**, 2202–2209 (2016)
23. Karaca, S., Atik, A.E., Elmaci, N., Yalcin, T.: Gas-phase structures and proton affinities of N-terminal proline containing b2+ ions from protonated model peptides. Int. J. Mass Spectrom. **393**, 1–8 (2015)
24. Bleiholder, C., Suhai, S., Harrison, A.G., Paizs, B.: Towards understanding the tandem mass spectra of protonated oligopeptides. 2: The proline effect in collision-induced dissociation of protonated Ala-Ala-Xxx-Pro-Ala (Xxx = Ala, Ser, Leu, Val, Phe, and Trp). J. Am. Soc. Mass Spectrom. **22**, 1032–1039 (2011)
25. Kuntz, A.F., Boynton, A.W., David, G.A., Colyer, K.E., Poutsma, J.C.: The proton affinity of proline analogs using the kinetic method with full entropy analysis. J. Am. Soc. Mass Spectrom. **13**, 72–81 (2002)
26. Boyd, R., Somogyi, A.: The mobile proton hypothesis in fragmentation of protonated peptides: A perspective. J. Am. Soc. Mass Spectrom. **21**, 1275–1278 (2010)
27. Dongre, A.R., Jones, J.L., Somogyi, A., Wysocki, V.H.: Influence of peptide composition, gas-phase basicity, and chemical modification on fragmentation efficiency: evidence for the mobile proton model. J. Am. Chem. Soc. **118**, 8365–8374 (1996)
28. Haeffner, F., Merle, J.K., Irikura, K.K.: N-protonated isomers as gateways to peptide ion fragmentation. J. Am. Soc. Mass Spectrom. **22**, 2222–2231 (2011)
29. Harrison, A.G.: Linear free energy correlations in mass spectrometry. J. Mass Spectrom. **34**, 577–589 (1999)
30. Paizs, B., Schnölzer, M., Warnken, U., Suhai, S., Harrison, A.G.: Cleavage of the amide bond of protonated dipeptides. Phys. Chem., Chem, Phys. **6**, 2691–2699 (2004)
31. Paizs, B., Suhai, S., Harrison, A.G.: Experimental and theoretical investigation of the main fragmentation pathways of protonated H-Gly-Gly-Sar-OH and H-Gly-Sar-Sar-OH. J. Am. Soc. Mass Spectrom. **14**, 1454–1469 (2003)
32. Frisch, M.J., Trucks, G.W., Schlegel, H.B., Scuseria, G.E., Robb, M.A., Cheeseman, J.R., Scalmani, G., Barone, V., Mennucci, B., Petersson, G.A., Nakatsuji, H., Caricato, M., Li, X., Hratchian, H.P., Izmaylov, A.F., Bloino, J., Zheng, G., Sonnenberg, J.L., Hada, M., Ehara, M., Toyota, K., Fukuda, R., Hasegawa, J., Ishida, M., Nakajima, T., Honda, Y., Kitao, O., Nakai, H., Vreven, T., Montgomery, J.A., Peralta, J.E., Ogliaro, F., Bearpark, M., Heyd, J.J., Brothers, E., Kudin, K.N., Staroverov, V.N., Keith, T., Kobayashi, R., Normand, J., Raghavachari, K., Rendell, A., Burant, J.C., Iyengar, S.S., Tomasi, J., Cossi, M., Rega, N., Millam, J.M., Klene, M., Knox, J.E., Cross, J.B., Bakken, V., Adamo, C., Jaramillo, J., Gomperts, R., Stratmann, R.E., Yazyev, O., Austin, A.J., Cammi, R., Pomelli, C., Ochterski, J.W., Martin, R.L., Morokuma, K., Zakrzewski, V.G., Voth, G.A., Salvador, P., Dannenberg, J.J., Dapprich, S., Daniels, A.D., Farkas, O., Foresman, J.B., Ortiz, J.V., Cioslowski, J., Fox, D.J.: Gaussian 09, Revision C.01. Gaussian, Inc, Wallingford (2010)
33. Zhao, Y., Truhlar, D.G.: The M06 suite of density functionals for main group thermochemistry, thermochemical kinetics, noncovalent interactions, excited states, and transition elements: two new functionals and systematic testing of four M06-class functionals and 12 other functionals. Theor. Chem. Acc. **120**, 215–241 (2008)
34. Zhao, Y., Schultz, N.E., Truhlar, D.G.: Exchange-correlation functional with broad accuracy for metallic and nonmetallic compounds, kinetics, and noncovalent interactions. J Chem. Phys. **123**(16), 161103 (2005)
35. Shi, L., Holliday, A.E., Shi, H., Zhu, F., Ewing, M.A., Russell, D.H., Clemmer, D.E.: Characterizing intermediates along the transition from polyproline I to polyproline II using ion mobility spectrometry-mass spectrometry. J. Am. Chem. Soc. **136**, 12702–12711 (2014)
36. Shi, L., Holliday, A.E., Bohrer, B.C., Kim, D., Servage, K.A., Russell, D.H., Clemmer, D.E.: "Wet" versus "dry" folding of polyproline. J. Am. Soc. Mass Spectrom. **27**, 1037–1047 (2016)
37. Shi, L., Holliday, A.E., Glover, M.S., Ewing, M.A., Russell, D.H., Clemmer, D.E.: Ion mobility-mass spectrometry reveals the energetics of intermediates that guide polyproline folding. J. Am. Soc. Mass Spectrom. **27**, 22–30 (2015)
38. Bythell, B.J., Barofsky, D.F., Pingitore, F., Polce, M.J., Wang, P., Wesdemiotis, C., Paizs, B.: Backbone cleavages and sequential loss of carbon monoxide and ammonia from protonated AGG: a combined tandem mass spectrometry, isotope labeling, and theoretical study. J. Am. Soc. Mass Spectrom. **18**, 1291–1303 (2007)
39. Bythell, B.J., Suhai, S., Somogyi, A., Paizs, B.: Proton-driven amide bond-cleavage pathways of gas-phase peptide ions lacking mobile protons. J. Am. Chem. Soc. **131**, 14057–14065 (2009)
40. Paizs, B., Suhai, S.: Combined quantum chemical and RRKM modeling of the main fragmentation pathways of protonated GGG. I. Cis-trans isomerization around protonated amide bonds. Rapid Commun. Mass Spectrom. **15**, 2307–2323 (2001)
41. Somogyi, A., Wysocki, V.H., Mayer, I.: The effect of protonation site on bond strengths in simple peptides: application of ab initio and modified neglect of differential overlap bond orders and modified neglect of differential overlap energy partitioning. J. Am. Soc. Mass Spectrom. **5**, 704–717 (1994)
42. El Aribi, H., Orlova, G., Hopkinson, A.C., Siu, K.W.M.: Gas-phase fragmentation reactions of protonated aromatic amino acids: concomitant and consecutive neutral eliminations and radical cation formations. J. Phys. Chem. A **108**, 3844–3853 (2004)
43. El Aribi, H., Rodriquez, C.F., Almeida, D.R.P., Ling, Y., Mak, W.W.N., Hopkinson, A.C., Siu, K.W.M.: Elucidation of fragmentation mechanisms of protonated peptide ions and their products: a case study on glycylglycylglycine using density functional theory and threshold collision-induced dissociation. J. Am. Chem. Soc. **125**, 9229–9236 (2003)
44. Rodriquez, C.F., Cunje, A., Shoeib, T., Chu, I.K., Hopkinson, A.C., Siu, K.W.M.: Proton migration and tautomerism in protonated triglycine. J. Am. Chem. Soc. **123**, 3006–3012 (2001)
45. Csonka, I.P., Paizs, B., Lendvay, G., Suhai, S.: Proton mobility in protonated peptides: a joint molecular orbital and RRKM study. Rapid Commun. Mass Spectrom. **14**, 417–431 (2000)
46. Jorgensen, T.J.D., Grdsvoll, H., Ploug, M., Roepstorff, P.: Intramolecular migration of amide hydrogens in protonated peptides upon collisional activation. J. Am. Chem. Soc. **127**, 2785–2793 (2005)
47. Ren, J., Tian, Y., Hossain, E., Connolly, M.: Fragmentation patterns and mechanisms of singly and doubly protonated peptoids studied by collision induced dissociation. J. Am. Soc. Mass Spectrom. **27**, 646–661 (2016)
48. Paizs, B., Suhai, S.: Towards understanding the tandem mass spectra of protonated oligopeptides. 1: Mechanism of amide bond cleavage. J. Am. Soc. Mass Spectrom. **15**, 103–113 (2004)
49. Nelson, C.R., Abutokaikah, M.T., Harrison, A.G., Bythell, B.J.: Proton mobility in b2 ion formation and fragmentation reactions of histidine-containing peptides. J. Am. Soc. Mass Spectrom. **27**, 487–497 (2016)